

Spectrally-selective mid-IR laser-induced inactivation of pathogenic bacteria

VICTOR KOMPANETS,¹ SVETLANA SHELYGINA,² ETERI TOLORDAVA,^{2,4}
SERGEY KUDRYASHOV,^{2,4} IRINA SARAEVA,^{2,4} ALEKSEY RUPASOV,² OLGA
BAITSAEVA,² ROMAN KHMELNITSKII,² ANDREY IONIN,² YULIA YUSHINA,⁴
SERGEY CHEKALIN,¹ AND MICHAEL KOVALEV^{5,*}

¹Institute of Spectroscopy, Russian Academy of Sciences, Troitsk, 108840 Russia

²Lebedev Physical Institute, Russian Academy of Sciences, Moscow, 119991 Russia

³Gamaleya National Research Center for Epidemiology and Microbiology, Moscow, 123098 Russia

⁴V.M. Gorbатов Federal Scientific Center for Food Systems, Russian Academy of Sciences, Moscow, 109316 Russia

⁵Bauman Moscow State Technical University, Moscow, 105005 Russia

*m.s.kovalev@bmstu.ru

Abstract: Micrometer-thick layers of *Pseudomonas aeruginosa* bacteria were prepared on fluorite substrates and scanned by focused mid-IR femtosecond laser radiation that was spectrally tuned to achieve the selective excitation of either the stretching C–H vibrations (3 μm), or stretching C=O, C–N vibrations (6 μm) of the amide groups in the bacteria. The enhanced biocidal efficiency of the latter selective excitation, comparing to the more uniform 3- μm laser excitation, was demonstrated by performing viability assays of laser-treated bacterial layers. The bacterial inactivation by the 6- μm ultrashort laser pulses is attributed to dissociative denaturation of lipids and proteins in the cell membranes and intra-cell nucleic acids.

© 2021 Optical Society of America under the terms of the [OSA Open Access Publishing Agreement](#)

1. Introduction

Exposure to ultraviolet (UV) radiation is the established method used to inactivate pathogenic microorganisms [1]. In general, UV radiation can be classified as short-wavelength (UVC, 200–280 nm), medium-wavelength (UVB, 280–315 nm), and long-wavelength (UVA, 315–380 nm) emission [1]. Regarding the disinfecting properties of UV radiation, pathological changes in deoxyribonucleic acid (DNA) molecules are caused by its photochemical reactions. The mutagenic effects of UVA and UVB are well known; UVA destroys DNA through oxidative stress, UVB causes direct DNA damage through the formation of cyclobutane-pyrimidine dimers and pyrimidine-(6-4)-pyrimidone photoproducts [2-4]. It is believed that such microorganism inactivation occurs through the UVC absorption-induced formation of cyclobutane dimers or pyrimidine photoproducts in the DNA chains. Exposure to small amounts of UV radiation causes double bonds in pyrimidine nitrogenous base molecules to break and instigates the formation of covalent bonds between adjacent nucleotides. It blocks DNA replication in cells [5]. As a result, UV irradiation renders microorganisms inactive rather than killing them outright [6, 7]. However, some species of UV-resistant bacteria are capable of DNA repair by expressing the DNA photolyase enzyme, which removes photoproducts and pyrimidine-pyrimidine dimers [8]. Photolyases are responsible for repairing various photoproducts and are found in most organisms; however, they are inactive or absent in mammals [6, 7]. The effects of absorbing UV radiation on human cells are well known: DNA is usually destroyed, leading to premature aging as well as the formation of mutations and burns, and, ultimately, can result in the development of melanoma. Hence, the use of UV light is limited.

46 Previously, Tsen et al. developed a method for inactivating bacteria and viruses based on
47 the use of femtosecond laser radiation at visible and near-IR wavelengths [9]. The authors
48 demonstrated that this method is effective regardless of the structure or mutational status of the
49 pathogen. With regard to viruses, inactivation is achieved by exciting mechanical vibrations of
50 the virus capsid, thereby causing bonds (specifically hydrogen bonds or hydrophobic contacts)
51 in the protein envelope of the virus to weaken and break, which inhibits the virus. The
52 mechanism underlying this process is known as impulsive stimulated Raman scattering and
53 involves the laser-induced excitation of low-frequency acoustic vibrations of the virus capsid.
54 For bacteria, relaxation occurs via the supercoiling of supercoiled DNA, which kills the
55 bacteria. This method is selective, chemical-free, and has minimal side effects. The therapeutic
56 window of laser radiation with power densities ranging from 1–10 GW/cm² enables the
57 inactivation of most pathogens without damaging mammalian cells. This method has shown
58 promise regarding the processing of blood products, pharmaceuticals, and vaccines [9].
59 Nevertheless, it also requires long exposure times and complex equipment, while its
60 effectiveness has been refuted in [10].

61 Infrared radiation can denature functional proteins in bacterial cells by destroying the
62 hydrogen bonds responsible for the stabilization of secondary and tertiary structures. Proteins
63 are essential components of all living organisms and perform functions important for cell
64 proliferation, with these functions realized through the activation of biocatalytic reactions,
65 electron transfer, and conformational transformations. In turn, secondary and tertiary structures
66 are fundamental for normal protein functions [11–13]. The migration and relaxation of
67 vibrational excitation energies in proteins have been studied in real time, using ultrafast
68 spectroscopy and mid-IR multiphoton vibrational excitation [14,15]. The effect of IR radiation
69 on the inactivation of pathogenic microorganisms has been studied previously [17,18]. For
70 example, Hamanaka et al. [17] investigated the effect of using thermal IR sources with different
71 wavelengths on the inactivation of bacterial spores with varying levels of water activity,
72 revealing that the maximum inactivation efficiency was achieved when using a source with a
73 wavelength of 950 nm. Elsewhere, Oduola et al. [18] demonstrated that the number of colony-
74 forming units of mold spores was reduced more effectively by using selective IR irradiation as
75 opposed to broadband IR irradiation. In addition, the authors reported that stationary IR
76 treatment had quite significant inactivation effect in the 6- μ m region, but was far less effective
77 in the 3- and 4.5- μ m regions.

78 Our previous studies have shown the strong perturbation of hydrogen bonds in the cells of
79 bacterial cultures of *Staphylococcus aureus* and *Pseudomonas aeruginosa* when exposed to
80 low-intensity (~ 0.1 – 10 GW/cm²) ultrashort pulses in the mid-IR range (5–6.6 μ m) in the region
81 of their characteristic absorption bands of proteins and lipids [19]. Specifically, our studies of
82 self-transmission of ultrashort laser pulses through a layer of separate bacteria cultivated on a
83 silicon substrate showed a relative bleaching in the region of these bands and their blue shift,
84 apparently indicating the breaking of hydrogen bonds. In the present work, we explicitly
85 evaluate the inactivation influence of mid-IR femtosecond laser radiation in the spectral ranges
86 of ~ 3 and 6 μ m on a micrometer-thick layer of a culture of pathogenic bacteria *Pseudomonas*
87 *aeruginosa*, followed by microbiological viability examination of the samples. Inactivation of
88 *Pseudomonas aeruginosa*, the Gram-negative pathogen and cause a wide range of human
89 diseases, is challenging because of the high resistance of the bacterium to antibiotics [20, 21].

90 **2. Methods**

91 **2.1 Experimental procedure**

92 A *Pseudomonas aeruginosa* culture was obtained from the Gamaleya National Research Center
93 for Epidemiology and Microbiology. The daily broth culture of 1 ml was centrifuged and the
94 supernatant was removed. Next, 1-ml volume of distilled water was added to the sediment and
95 shaken intensively. The resulting suspension was diluted by serial decimal dilutions up to 10^5
96 CFU/ml. The bacterial culture was dripped onto the CaF₂ substrates in a volume of 100 μ l and

97 dried for 10-15 minutes. Micrometer-thick (average thickness $\approx 1.5 \mu\text{m}$ measured in a contact
 98 mode, using an atomic force microscope Certus Standart) layers of the *P. aeruginosa* culture,
 99 consisting of sub-micron-wide and a few-micron long bacteria [22], were prepared on 2-mm-
 100 thick CaF_2 plates, which have 90% transmittance in the 0.15–9.0 μm range.

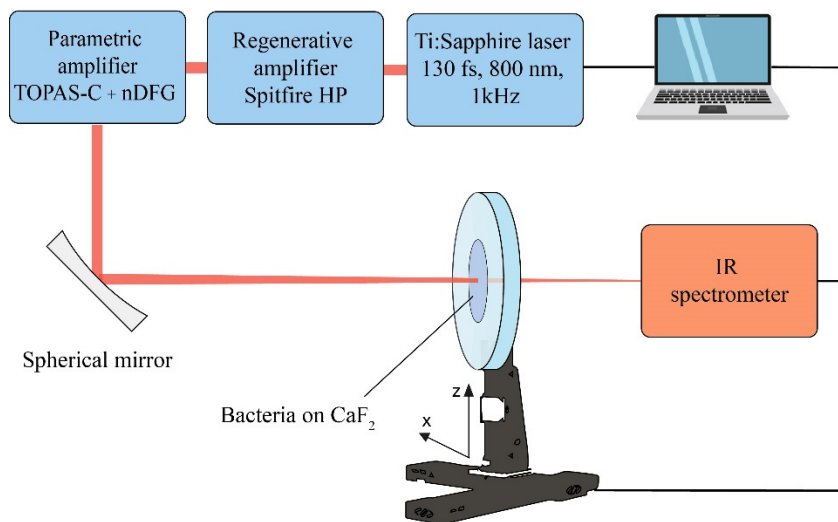


Fig. 1. Schematic diagram of the experimental set-up.

101
 102

103 The micro-layer samples of the *P. aeruginosa* culture were exposed to femtosecond laser
 104 pulses at two wavelengths, corresponding to the characteristic vibrations of proteins and fatty
 105 acids in bacterial cells. As shown in Fig. 1, the samples were placed in front of the entrance slit
 106 of the IR-spectrometer (Solar TII MS2004) along the normal to the optical axis of radiation.
 107 The incident laser light was focused on the slit by a spherical mirror with a focal length of 150
 108 mm. Mid-IR laser irradiation (central wavelength: 5.8 μm , FWHM: 0.6 μm ; central wavelength:
 109 $\approx 3.4 \mu\text{m}$, FWHM $\approx 0.4 \mu\text{m}$) with the FWHM pulse duration $\tau \approx 130$ fs, maximum pulse energies
 110 of 10 μJ (6 μm) and 30 μJ (3 μm), and the repetition rate of 1 kHz was obtained via parametric
 111 generation using a Ti:sapphire laser (Spitfire HP, Spectra-Physics, central wavelength: 800 nm,
 112 frequency: 1 kHz, FWHM: 50 fs) and an optical parametric amplifier (OPA) with a difference-
 113 frequency module (OPA TOPAS-C + nDFG, Light Conversion) [19].

114 These particular wavelengths were selected in accordance with the characteristic vibrations
 115 of the C–N and C=O bonds of amides (1510–1700 cm^{-1} , $\approx 6 \mu\text{m}$), the C–H bond of fatty acids,
 116 and the N–H bond of amides (~ 3100 – 3500cm^{-1} , $\approx 3 \mu\text{m}$) (Fig. 2) [23]. The peak intensity ranges
 117 of the 6- μm and 3- μm ultrashort laser pulses are $I_0 = 0.18$ – $1.1 \text{ TW}/\text{cm}^2$ and 0.07 – $8 \text{ TW}/\text{cm}^2$,
 118 respectively. The peak intensity was changed by moving the samples along the optical axis to
 119 change the size of the irradiation area (defocusing). The beam diameter was measured using a
 120 scanning slit beam profiler. All beam diameters were measured at the FWHM and ranged from
 121 60 to 640 μm and from 88 to 224 μm at the wavelengths of 3 μm and 6 μm , respectively. The
 122 samples were raster-scanned with 50% overlapping ($N = 2$ shots/spot), using a software-
 123 controlled motorized two-coordinate translation stage and making 3 series with new samples
 124 for each set of laser-irradiation conditions. Stationary spectra of the optical density (from 400–
 125 4000 cm^{-1}) were obtained using a Fourier-transform infrared (FT-IR) spectrometer (Vertex V-
 126 70, Bruker).

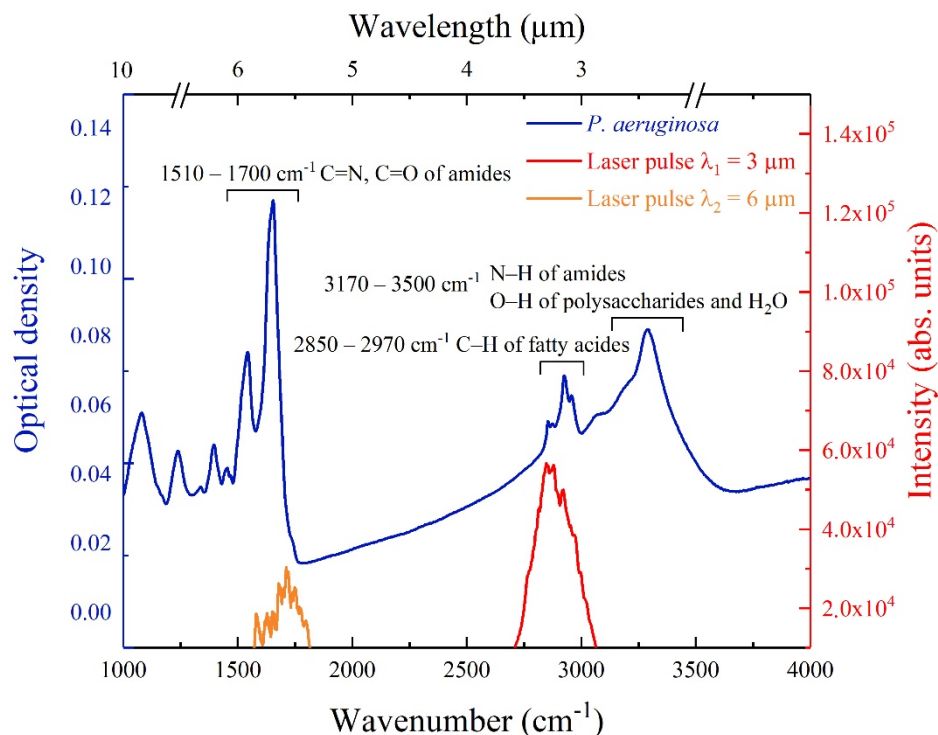


Fig. 2. FT-IR optical density spectrum of 1.5-micrometer thick layer of *P. aeruginosa* bacteria (left axis, spectral assignment after [24,25]) shown in relation to the intensity spectra of the 3- μm and 6- μm laser pulses (right axis).

128

129

130

131

132

2.2 Viability assays

133

134

135

136

137

138

139

140

141

After laser exposure, the entire laser-treated and control substrates were moved to individual sterile tubes with saline solution and shaken intensively for 30 minutes. The resulting suspension was sown on dense nutrient medium and placed in a thermostat for one day at 37 °C. A day later, the bacterial colony was counted to determine the number of colony forming units (CFUs) and recalculated to CFU/ml values. The obtained *P. aeruginosa* values were compared with the control samples that were not exposed to the laser (Fig. 3). The decrease in the CFU/ml value for *Pseudomonas aeruginosa* by 2-3 or more orders of magnitude showed that the method has a pronounced antibacterial effect. In the future, such multi-parametric experiments will be performed for a wide range of microorganisms with multiple repetitions.

142

3. Results

143

3.1 Bacterial inactivation

144

145

146

147

148

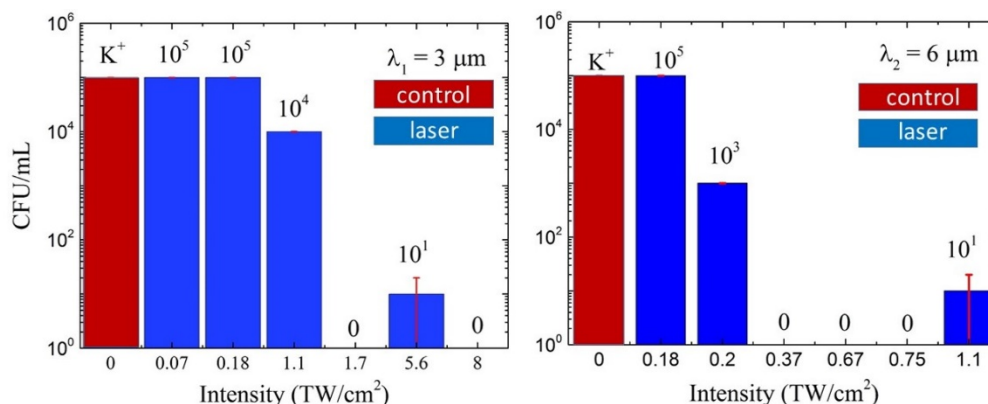
149

150

151

The results of the viability assays showed the threshold-like, distinct and significant intensity-dependent reduction in the number of CFUs for the samples of the *P. aeruginosa* culture exposed by the 6- μm laser radiation (Fig. 3, right). The threshold value, where the CFU number reduction (*not total sterilization!*) becomes evident, was evaluated as $0.3 \pm 0.1 \text{ TW/cm}^2$. In contrast, for the *P. aeruginosa* samples exposed by the femtosecond laser radiation at the wavelength of 3 μm , changes in the number of CFUs were rather negligible until $1.4 \pm 0.3 \text{ TW/cm}^2$ (Fig. 3, left). It should be noted that previous CW studies on the mid-IR treatment of bacteria also showed efficient inactivation for the 6- μm region, but not in the 3- and 4.5- μm

152 spectral regions [26]. For both these 3- μm and 6- μm exposures, at the above-threshold laser
 153 intensities the bacterial abundance decreases by 4-5 orders of magnitude regarding the control,
 154 thus indicating the definite disinfection of the fluorite substrates. Potentially, such MIR-laser
 155 sterilization is possible too, but some technical difficulties, as scan line stitching and interline
 156 sub-threshold exposure should be solved, resulting in the artifact residual bacterial presence
 157 (~ 10 CFU/ml) at higher above-threshold intensities in Fig. 3.
 158



159
 160 **Fig. 3.** CFU numbers versus laser intensity at the wavelengths of 3 μm (left) and 6 μm (right);
 161 K^+ is the control sample. The minor residual bacterial presence at higher intensities is the
 162 technical artifact of incomplete stitching of laser scan lines at the reduced focal size and the
 163 threshold-like bacteria inactivation.

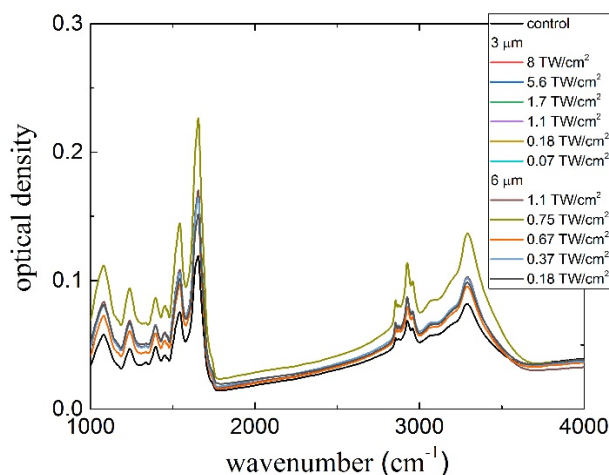
164 As shown in Fig. 2 in the FT-IR spectrum of *P. aeruginosa* bacteria, the 6- μm laser pulses
 165 (wavenumbers in the range of 1650–1750 cm^{-1}) hit their characteristic vibrational bands,
 166 corresponding to 1) $>\text{C}=\text{O}$ -bond in nucleic acids (1680–1715 cm^{-1}), 2) $\text{C}=\text{O}$ stretching
 167 vibrations of ester functional groups from lipids and fatty acids (~ 1740 cm^{-1}), and 3) $\text{C}=\text{O}$
 168 stretching vibrations of amides associated with α - and β - protein structures (amide I band: 1650
 169 cm^{-1}), through very intense local excitation. In contrast, the 3- μm laser pulses (wavenumber
 170 spectrum of 2700–3050 cm^{-1} , Fig. 2) can hit the only $\text{C}-\text{H}$ asymmetric stretching vibration in
 171 $-\text{CH}_2$ and $-\text{CH}_3$ fragments of fatty acids and lipids in the bacterial cell wall in the range of 2800–
 172 3000 cm^{-1} [24, 25], providing rather homogeneous excitation of the bacteria, but requiring for
 173 the inactivation much higher laser intensities.

174 3.2 Local “effective” temperatures in bacteria

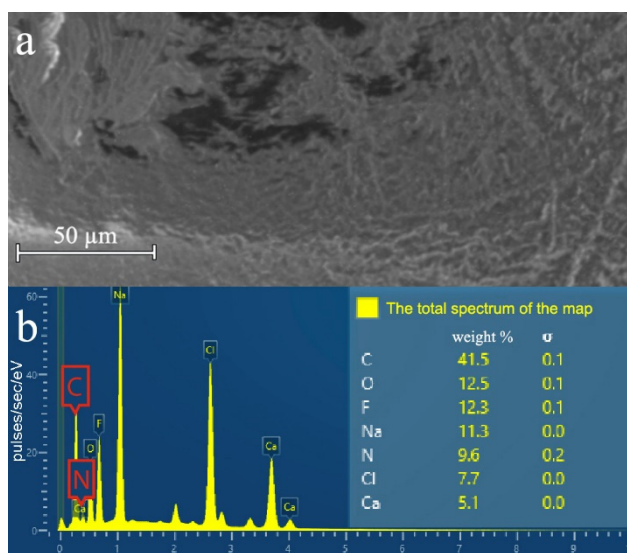
175 In the context of the strongly different MIR-laser bacterial inactivation thresholds at the 3- μm
 176 and 6- μm laser wavelength, we were tempted to investigate the underlying reasons. First, based
 177 on the pre- and post-irradiation FTIR spectroscopic optical density measurements (see, e.g.,
 178 Fig. 4), as well as optical visual/microscopic inspections, we can exclude global ablation of the
 179 bacteria from the substrate (catapulting [27]) or local ablation of the walls. The internal laser
 180 ablation inside the cells could be considered as a dissociation process, while we can’t
 181 distinguish non-equilibrium and equilibrium dissociation in non-thermalized and thermalized
 182 molecules, respectively, but can evaluate the driving “effective” local temperatures. Moreover,
 183 the condensed matter environment in the bacterial cells enables to distinguish thermalization
 184 and heat-conduction stages in the intracellular vibrational dynamics, where for the multi-
 185 micron focal spots we will neglect by the latter millisecond stage on the inactivation scale for
 186 the low thermal conductivity value of water, being the main component of the intracellular
 187 fluid.

188 First, we evaluated the local MIR-absorption effects in the *P. aeruginosa* bacteria at the 3-
 189 μm and 6- μm laser wavelengths. According to the FT-IR optical density spectrum in Fig. 2, the
 190 average extinction coefficient over the 1.5-micron thick bacterial layer measured by atomic

191 force microscopy, is $\kappa_6 \approx 8 \times 10^2 \text{ cm}^{-1}$ at the 6- μm wavelength for the amide groups of proteins
 192 and nucleic acids versus $\kappa_3 \approx 40 \text{ cm}^{-1}$ for the C-H groups at the 3- μm wavelength. Second, we
 193 accounted for the local distribution of the amide groups in the bacteria. For this purpose, we
 194 used energy-dispersive X-ray (EDX) analysis (Fig. 5) to measure the molar ratio C:N as the
 195 number of C-N (local absorption) and C-H (almost uniform absorption) vibrations in the
 196 bacterial cells, determined as 5 for their weight ratio 41.5:9.6 and the nearly even molar masses
 197 $M_C = 12 \text{ g/mole}$ and $M_N = 14 \text{ g/mole}$ (Fig. 5), respectively. Hence, the effective extinction
 198 coefficient of the amide groups at the 6- μm wavelength can be increased five-fold till
 199 $\kappa_6^* \approx 4 \times 10^3 \text{ cm}^{-1}$, i.e., two orders of magnitude higher, than at the at the 3- μm wavelength. As a
 200 result, one can anticipate much stronger spectrally and spatially selective 6- μm absorption and
 201 vibrational excitation for the amide groups in the bacteria (Fig. 6), than the uniform 3- μm
 202 absorption by C-H bonds.
 203



204
 205 **Fig. 4.** FT-IR optical density spectra of 1.5-micrometer thick layer of *P. aeruginosa* bacteria
 206 upon 3- μm and 6- μm fs-laser exposures at different intensities, shown in the frame.
 207

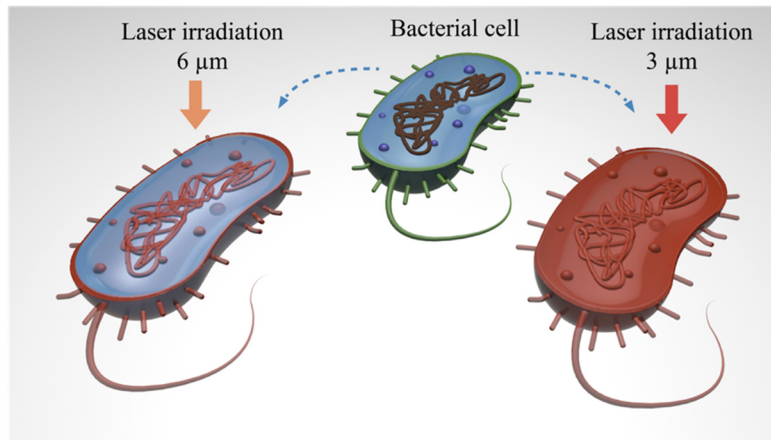


208
 209 **Fig. 5.** (a) Top-view scanning electron microscope image of the micron-thick *P. aeruginosa*
 210 layer on the CaF_2 substrate and (b) the corresponding 10-keV EDX spectrum and datasheet,
 211 including also the contribution of the CaF_2 substrate.

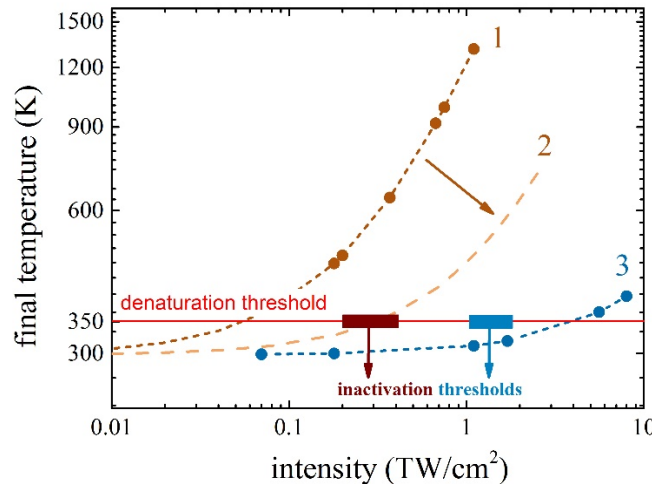
212 Finally, the intensity dependence of the elevated bacterial temperature was calculated for
 213 the 2 pulse/spot exposures at the 1-kHz repetition rate (Fig. 7), using the experimental (I_0 , τ ,
 214 $N=2$) and derived (κ_3, κ_6^*) parameters for the bacterial heat capacity, approximated by that one
 215 for water ($C_p \approx 1.3 \text{ J/cm}^3\text{K}$), as follows

$$216 \quad T(I_0, \lambda) = T_\infty + N \frac{\kappa_\lambda^* I_0 \tau}{C_p}. \quad (1)$$

217 The calculated dependences demonstrate the much stronger temperature rise for the more
 218 selective 6- μm heating, which could result in *P. aeruginosa* inactivation above the protein
 219 denaturation threshold temperature of $\approx 80 \text{ }^\circ\text{C}$ (350 K) [28], where for the most of proteins,
 220 denaturation is irreversible. The much higher effective absorption coefficient at the 6- μm
 221 wavelength anticipates the corresponding much lower threshold intensity for the bacterial
 222 inactivation (Fig. 3).
 223



224
 225 **Fig. 6.** Schematic representation of the local and global absorption/vibrational excitation/heating
 226 effects of laser radiation at the wavelengths of 3 μm and 6 μm , respectively, on the bacterial
 227 cells.



228
 229 **Fig. 7.** Calculated dependences of effective bacterial temperature as a function of the
 230 femtosecond laser intensity at the wavelengths of 6 (curves 1,2) and 3 (curve 3) μm . The color
 231 symbols indicate the experimental intensity values, and the inactivation threshold intensities

232
233
234
235
236

(color rectangles with the arrows) corresponds to the onset of CFU reduction in Fig. 3. The curves 1 and 2 differ by the factor of intramolecular energy transfer (≈ 5.5), derived to fit the 6- μm inactivation threshold intensity to the denaturation threshold temperature for most of proteins $\approx 80\text{ }^\circ\text{C}$ (350 K). Such intramolecular energy transfer factor in the case of uniform heating by the 3- μm radiation is negligible.

237
238
239
240
241
242
243
244
245
246
247

However, the calculated denaturation threshold intensity at the 6- μm wavelength ($\approx 0.06\text{ TW/cm}^2$) exceeds almost five-fold the experimentally measured inactivation threshold of $\approx 0.3\text{ TW/cm}^2$ (Fig. 3). This apparently indicates the considerable intramolecular (*but almost not inter-molecular!*) energy transfer around the local absorbing amide groups almost naturally down to the uniform heating (cf., the EDX-derived factor of 5 above for the density of local C-N and highly-abundant C-H vibrations in the bacteria). As a result, the temperature dependence calculated for the 6- μm wavelength (curve 1) was scaled down in Fig. 7 by this factor (curve 2). Meanwhile, the large handicap in the effective absorption coefficient between the 3- μm and 6- μm wavelengths still results in much higher inactivation threshold, as predicted by our calculations and the resulting curve 3 in Fig. 7.

248

4. Conclusion

249
250
251
252
253
254
255
256
257
258
259
260
261
262

In this study, we investigated the efficiency of selective and non-selective femtosecond mid-IR (3 μm and 6 μm) laser irradiation with respect to the inactivation of the pathogenic *P. aeruginosa* bacteria. Microbiological viability studies demonstrated that rather uniform femtosecond laser-induced vibrational excitation of the bacteria at 3- μm wavelength corresponds to \approx five-fold higher intensity threshold for the efficient bacterial inactivation, comparing to the more spatially-selective excitation by femtosecond laser pulses at the 6- μm wavelength. In the latter case, the laser irradiation apparently causes hydrogen bonds in the secondary and tertiary structure of bacterial proteins to break and damages the DNA of the bacteria via non-equilibrium or equilibrium (thermal) dissociation. Owing to the strong absorption of 6- μm laser radiation by proteins and lipids, the anticipated effective temperature rise in the cells even after intense intramolecular energy transfer is significantly higher, than for the 3- μm irradiation, resulting in the irreversible denaturing of proteins and nucleic acids in the bacterial cells. The proposed approach appears to be promising for antibacterial treatment and, potentially, sterilization in medical and industrial food environments.

263

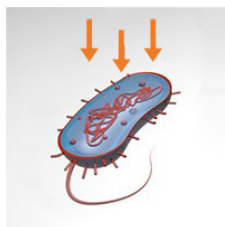
Funding. Ministry of Science and Higher Education of the Russian Federation (075-15-2020-775).

264

Disclosures. The authors declare no conflicts of interest.

265
266

Data availability. The data underlying the results presented in this paper are available from the authors upon reasonable request.



267
268

Fig. 2. Preview of thumbnail image display on the author submission page.

269

References

270
271
272
273
274

1. J.K. Setlow "The effects of ultraviolet radiation and photoreactivation," *Compr. Biochem.* **27**, 157–209 (1967).
2. J. Jagger, "Near-UV radiation effects on microorganisms," *Photochem Photobiol.* **34**, 761–768 (1981)
3. A. Svobodova, A. Galandakova, J. Sianska, D. Dolezal, R. Lichnovska, J. Ulrichova, J. Vostalova, "DNA damage after acute exposure of mice skin to physiological doses of UVB and UVA light," *Arch Dermatol Res* **304**(5), 407–412 (2012)

- 275
276
277
278
279
280
281
282
283
284
285
286
287
288
289
290
291
292
293
294
295
296
297
298
299
300
301
302
303
304
305
306
307
308
309
310
311
312
313
314
315
316
317
318
319
320
321
322
323
324
325
326
327
328
329
330
331
332
4. R. P. Sinha and D. Häder, "UV-induced DNA damage and repair: a review," *Photochem. Photobiol. Sci.* **1**(4), 225–236 (2002).
 5. R. B. Webb and M. J. Peak, "The effect of stray light in the 300–320-nm range and the role of cyclobutyl pyrimidine dimers in 365-nm lethality" *Mutat. Res.* **91**(3), 1770–1782 (1981).
 6. C. Jungfer, T. S. Å, and U. Obst, "UV-induced dark repair mechanisms in bacteria associated with drinking water," *Water Res.* **41**, 188–196 (2007).
 7. C. Auerbach, "Mutagenesis problems" (Moscow, Mir, 1978) [in Russian].
 8. A. Yasui, A. P. M. Eker, S. Yasuhira, H. Yajima, T. Kobayashi, M. Takao, and A. Oikawa, "A new class of DNA photolyases present in various organisms including aplacental mammals," *EMBO J.* **13**(24), 6143–6151 (1994).
 9. S. W. D. Tsen, T. C. Wu, J. G. Kiang, and K. T. Tsen, "Prospects for a novel ultrashort pulsed laser technology for pathogen inactivation," *J. Biomed. Sci.* **19**, 62 (2012).
 10. J. C. Wigle, E. A. Holwitt, L. E. Estlack, G. D. Noojin, K. E. Saunders, V. V. Yakovlev, and B. A. Rockwell, "No effect of femtosecond laser pulses on M13, *E. coli*, DNA, or protein," *J. Biomed. Opt.* **19**(1), 015008 (2014).
 11. D. C. Elliott and E. W. Elliott, *Biochemistry and Molecular Biology*, 2nd ed. (Oxford University Press, 2001).
 12. V. S. Letokhov, "Photophysics and Photochemistry," *Phys. Today* **30**(5), 23–32 (1977).
 13. D. Laage, T. Elsaesser, and J. T. Hynes, "Water Dynamics in the Hydration Shells of Biomolecules," *Chem. Rev.* **117**(16), 10694–10725 (2017).
 14. E. H. G. Backus, P. H. Nguyen, V. Botan, R. Pfister, A. Moretto, M. Crisma, C. Toniolo, G. Stock, and P. Hamm, "Energy transport in peptide helices: A comparison between high- and low-energy excitations," *J. Phys. Chem. B* **112**(30), 9091–9099 (2008).
 15. L. P. DeFlores, Z. Ganim, S. F. Ackley, H. S. Chung, and A. Tokmakoff, "The anharmonic vibrational potential and relaxation pathways of the amide I and II modes of N-methylacetamide," *J. Phys. Chem. B* **110**(38), 18973–18980 (2006).
 16. C. Kolano, J. Helbing, M. Kozinski, W. Sander, and P. Hamm, "Watching hydrogen-bond dynamics in a β -turn by transient two-dimensional infrared spectroscopy," *Nature* **444**, 469–472 (2006).
 17. D. Hamanaka, T. Uchino, N. Furuse, W. Han, and S. ichiro Tanaka, "Effect of the wavelength of infrared heaters on the inactivation of bacterial spores at various water activities," *Int. J. Food Microbiol.* **108**(2), 281–285 (2006).
 18. A. A. Oduola, R. Bowie, S. A. Wilson, Z. Mohammadi Shad, and G. G. Atungulu, "Impacts of broadband and selected infrared wavelength treatments on inactivation of microbes on rough rice," *J. Food Saf.* **40**(2), e12764 (2020).
 19. V. O. Kompanets, S. I. Kudryashov, E. R. Totordava, S. N. Shelygina, V. V. Sokolova, I. N. Saraeva, M. S. Kovalev, A. A. Ionin, and S. V. Chekalin, "Femtosecond infrared laser spectroscopy of characteristic molecular vibrations in bacteria in the 6- μ m spectral range," *JETP Lett.* **113**(6), 365–369 (2021).
 20. Z. Pang, R. Raudonis, B. R. Glick, T. J. Lin, and Z. Cheng, "Antibiotic resistance in *Pseudomonas aeruginosa*: mechanisms and alternative therapeutic strategies," *Biotechnol. Adv.* **37**(1), 177–192 (2019).
 21. N. J. Palleroni, "Human- and animal-pathogenic pseudomonads," in *The Prokaryotes*, (Springer-Verlag: New York, 1992).
 22. A. A. Nastulyavichus, S. I. Kudryashov, E. R. Tolordava, L. F. Khaertdinova, Y. K. Yushina, T. N. Borodina, S. A. Gonchukov, and A. A. Ionin "Dynamic light scattering detection of silver nanoparticles, food pathogen bacteria and their bactericidal interactions," *Laser Phys. Lett.*, **18**(8), 086002 (2021).
 23. V. O. Kompanets, V. N. Lokhman, D. G. Poydashev, S. V. Chekalin, and E. A. Ryabov, "Dynamics of photoprocesses induced by femtosecond infrared radiation in free molecules and clusters of iron pentacarbonyl," *J. Exp. Theor. Phys.* **122**(4), 621–632 (2016).
 24. X. Lu, H. M. Al-Qadiri, M. Lin, and B. A. Rasco, "Application of mid-infrared and Raman spectroscopy to the study of bacteria," *Food Bioprocess Technol.* **4**(6), 919–935 (2011).
 25. H. M. Al-Qadiri, M. A. Al-Holy, M. Lin, N. I. Alami, A. G. Cavinato, and B. A. Rasco, "Rapid detection and identification of *Pseudomonas aeruginosa* and *Escherichia coli* as pure and mixed cultures in bottled drinking water using fourier transform infrared spectroscopy and multivariate analysis," *J. Agric. Food Chem.* **54**(16), 5749–5754 (2006).
 26. X. Lu, Q. Liu, D. Wu, H. M. Al-Qadiri, N. I. Al-Alami, D. H. Kang, J. H. Shin, J. Tang, J. M. F. Jabal, E. D. Aston, and B. A. Rasco, "Using of infrared spectroscopy to study the survival and injury of *Escherichia coli* O157:H7, *Campylobacter jejuni* and *Pseudomonas aeruginosa* under cold stress in low nutrient media," *Food Microbiol.* **28**(3), 537–546 (2011).
 27. S. Shukla, S. Kudryashov, K. Lyon, and S. D. Allen "Dry and wet laser catapulting and ablation of cells and bacteria by nanosecond CO₂ laser," *Proc. SPIE* **6084**, 608417 (2006).